Received March 20, 2019, accepted April 3, 2019, date of publication April 9, 2019, date of current version May 1, 2019.

Digital Object Identifier 10.1109/ACCESS.2019.2909911

Subblocks Set Design Aided Orthogonal Frequency Division Multiplexing With All Index Modulation

YUXIN SHI, XINJIN LU, KAI GAO, JIANG ZHU, AND SHILIAN WANG
College of Electronic Science, National University of Defense Technology, Changsha 410073, China
Corresponding author: Kai Gao (gaokai000@hotmail.com)

ABSTRACT In recent years, OFDM with index modulation (OFDM-IM) has become a potential technique due to its improvement of diversity gain. In typical OFDM-IM schemes, incoming information bits are divided into two parts, symbols bits, and index bits. However, the symbol bits conveyed by each OFDM symbol suffer from low diversity order, which has a negative impact on diversity gain. In this paper, we propose the scheme called OFDM with all index modulation (OFDM-AIM), which replaces the PSK/QAM constellation modulator with subblock modulator and simplifies the structure. With such an arrangement, the subblocks of OFDM-AIM become flexible, which contributes to achieving the higher diversity order of the system. Moreover, we study the effects of Euclidean distance and diversity order based on the unconditional pair error probability, which gives the guideline to design a legitimate subblocks set. Then the algorithm to build the subblocks set with higher diversity order is proposed, which can achieve better diversity gain. Theoretical and simulated results show that the OFDM-AIM scheme is capable of achieving better BER performance than other index modulated OFDM schemes.

INDEX TERMS OFDM-IM, diversity order, diversity gain, all index modulation, Euclidean distance, subblocks set design, pairwise error probability.

I. INTRODUCTION

Orthogonal-frequency division multiplexing (OFDM), has been widely used in wireless communications as a classical technique due to its high utilization of frequency, high spectral efficiency and simple system of one-tap equalization [1]. With these distinctive advantages, OFDM is accepted by many wireless communication standards, such as long-term evolution (LTE) [2], wireless fidelity (Wi-Fi) [3] and the worldwide interoperability for microwave access (WiMAX) [4]. In the standards of LTE, OFDM is regarded as core technique in downlink transmission [5]. OFDM can be also combined with a multiple-input multiple output (MIMO) techniques with design of antenna arrays to enhance the system capacity and diversity order [6]. Recently, index modulation (IM) has become a potential technique, which relies on the index of some medium to achieve better performance on transmission [7]. The advantages of Index modulation meet the escalating teletraffic and energy consumption, which has necessitated the development of green communication techniques [8]. This technique successfully transplanted the index concept from the antenna of Spatial Modulation (SM) technique [9] to subcarriers of OFDM in frequency domain.

A subcarrier-index modulated OFDM (SIM) [10] and an enhanced SIM-OFDM scheme (ESIM-OFDM) [11] are proposed, which can obtain some diversity gain compared to classical OFDM. However, the spectral efficiency (SE) is limited due to the fixed system models. In [12], OFDM-IM is proposed where the flexible system model meets the requirement of different SEs. Moreover, the relationship between subcarrier activation patterns (SAPs) and information conveyed by SAPs is presented by look-up table and combinatorial method. To achieve higher SE, two generalized OFDM-IM schemes called (GIM-OFDM) are proposed to permit more legitimate indices combination and expand the index domain to the both in-phase and quadrature (I/Q) components [13]. Low-complexity detector based on maximum-likelihood (ML) and OFDM-I/Q-IM is proposed in [14]. However, the performance is still reduced in high SE requirements due to the idle subcarriers, which does

The associate editor coordinating the review of this manuscript and approving it for publication was Irfan Ahmed.

not carry any symbol bits, resulting in the higher order QAM/PSK constellation points in active subcarriers. In [15], dual-mode OFDM-IM (DM-OFDM-IM) is proposed where idle subcarriers are replaced by the other distinguishable constellation alphabets, which fully uses the spectrum to adapt high SE transmission cases. Then DM-OFDM-IM is combined with GIM, called GDM scheme [16]. However, symbol bits containing the lowest diversity order in DM-OFDM-IM scheme still take a large proportion of all the incoming information bits, which limits its diversity gain. Then dual constellation alphabets with addition of zero are considered to achieve better performance than DM-OFDM-IM [17]. In multiple mode index modulation scheme (MM-OFDM-IM) [18], multiple modes are introduced to the system, which introduces more index bits and increases the proportion of index bits. To increase the bit error rate (BER) performance in frequency selective fading channel, simple and efficient interleaver is conducted in [19], which has been widely used in index modulated OFDM schemes. In coodinary interleaved OFDM-IM (CI-OFDM-IM) [20], where the real and imaginary parts of two OFDM symbols are interleaved after using the rotated constellation set, the diversity order of the system in CI-OFDM-IM is larger than 1. With the arrangement of searching the optimal rotation angle, the enhancement of BER is achieved. Further, the achievable performance of OFDM-IM has been studied in [21]. Inspired by [22] and [23], linear constellation precoding (LCP) technique is used to harvest additional diversity gain in [24]. Recently, coordinate interleaving [20], linear precoding technique [24] and MM-OFDM-IM [18] are combined in [25], which aims to obtain high diversity gain and high SE. In [26], coded OFDM-IM is proposed to achieve a diversity gain for index detection at the cost of the spectral efficiency. Subsequently, the indices of active subcarriers are replaced with indices of spreading codes in [27], which enhances the diversity order compared to OFDM-IM. In [28], repeated M-ary symbols are used in OFDM-IM to enhance the diversity order of the system. In [29], precoding matrices such as Walsh-Hadamard (WH) and Zadoff-Chu (ZC) are utilized in order to spread the symbols and indices, which increases the transmit diversity.

However, the diversity order is not fully obtained by most of the index modulated schemes, where the diversity order of system is only larger than 2 in some enhanced OFDM-IM schemes. In other words, the structure of index modulation in OFDM limits the diversity order of the system, which does not fully attain high diversity gains.

Against the background, we propose a new scheme called OFDM with all index modulation (OFDM-AIM) with the focus on achieving the diversity gain. In this paper, we simplify the structure of typical index modulated OFDM schemes and remove all of the symbol bits. With such arrangement, the subblocks become more flexible and thus the diversity order can be increased by the design of the subblocks set with higher diversity order. Moreover, the relationship between Euclidean distance and diversity order is discussed in this paper, which provides the guidelines of designing the subblocks set. According to the guidelines, the subblocks set composed by repeated vectors with the highest diversity order and the algorithm to search the subblocks with higher diversity order are proposed, which attains the better BER performance.

The rest of the paper is organized as follows: Section II reviews the typical index modulated OFDM schemes, where the structure and diversity order are discussed. The system model of OFDM-AIM is presented at Section III. In Section IV, the guidelines to build the legitimate subblocks set are proposed based on the pairwise error probability (PEP) events. After that, the algorithm of searching the subblocks set is given in Section V. The simulation results and theoretical upper bound based on union bound are presented at Section VI. In Section VII, the paper is concluded.

Notation: $\mathcal{X} \sim \mathcal{CN}(0, \sigma^2)$ represents the distribution of a circularly symmetrical complex Gaussian random variable $\mathcal{X}$ with the variance σ^2. $\lfloor\cdot\rfloor$ and $\lceil\cdot\rceil$ are the floor and ceiling operation respectively. I_N denotes the $N \times N$ dimension identity matrix. $(\cdot)^T$ and $(\cdot)^H$ denote Hermitian transpose and transpose. $Q(\cdot)$ denotes the tail probability of the standard Gaussian distribution. rank(X) returns the rank of a matrix X. $diag(x)$ creates a diagonal matrix whose diagonal elements are x. $\|\cdot\|_F$ denotes Frobenius-norm of a matrix.$\|\cdot\|_2$ denotes 2-norm of a vector.

II. REVIEW OF TYPICAL INDEX MODULATED OFDM SCHEMES

A. SYSTEM MODEL OF TYPICAL INDEX MODULATED OFDM SCHEMES

In this section, three typical index modulated OFDM schemes, OFDM-IM, DM-OFDM-IM and MM-OFDM-IM are illustrated in Fig. 1. A total of m information bits are purposed to transmitted by OFDM system each time. These m bits are split into g groups, each containing p bits. Each p bits are mapped to a OFDM subblock comprised by n subcarriers. When incoming p bits for each subblock, $p_1$bits called index bits are used to determine the index in look-up table whilst p_2 bits called symbols bits are mapped to OFDM symbols by M-ary QAM/PSK modulator. In each subblock, subcarriers are modulated by two different constellation alphabets S_A and S_B ($S_A \wedge S_B = \emptyset$) in OFDM-IM and DM-OFDM-IM whilst the number of the constellation alphabets in MM-OFDM-IM is more than 2 such as S_A, S_B and S_C. For OFDM-IM, S_A or S_B equals 0, whilst for DM-OFDM-IM and MM-OFDM-IM, none of the constellation alphabets equals 0. In Table 1, the look-up table which provides the indices of different SAPs for corresponding $p_1$bits is presented, where $s_A \in S_A$, $s_B \in S_B$ and $s_C \in S_C$ are the SAPs of each OFDM symbols. After the operation of M-ary QAM/PSK modulator, the OFDM symbols of each subblock are finally determined by p_2 bits.

By OFDM block creator, the g subblocks are combined into N OFDM symbols in frequency domain, given by

$$x_F = [x_F(1)\, x_F(2)\, , \ldots , x_F(N)]^T , \tag{1}$$

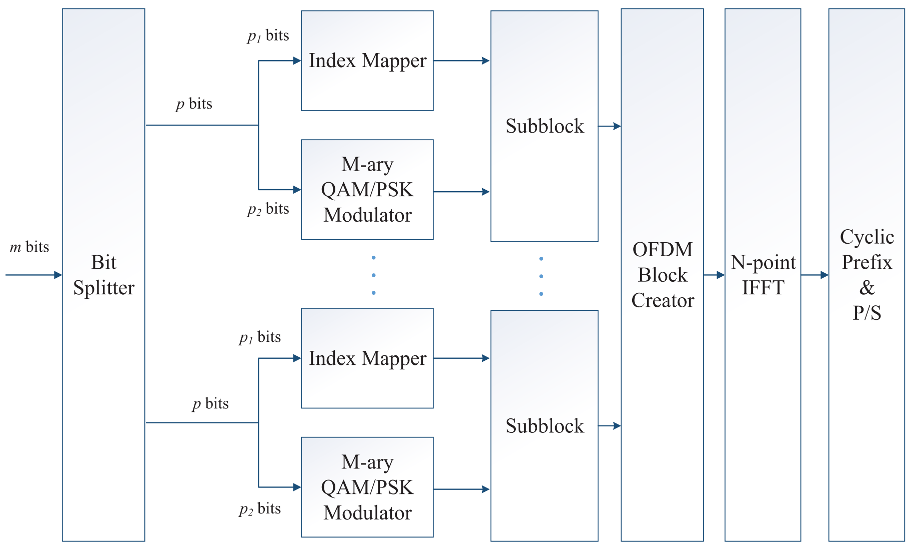

FIGURE 1. Block diagram of OFDM-IM transmitter.

TABLE 1. The look-up table of typical index modulated OFDM.

$p_1 bits$	SAPs of OFDM-IM/DM-OFDM-IM	SAPs of MM-OFDM-IM
00	$[s_A\ s_A\ s_B\ s_B\ ]$	$[s_A\ s_B\ s_C\ ]$
01	$[s_B\ s_A\ s_A\ s_B\ ]$	$[s_B\ s_A\ s_C\ ]$
10	$[s_B\ s_B\ s_A\ s_A\ ]$	$[s_B\ s_C\ s_A\ ]$
11	$[s_A\ s_B\ s_B\ s_A\ ]$	$[s_A\ s_C\ s_B\ ]$

Then the signals in time domain can be represented by inverse FFT (IFFT) operation. Similarly in classical OFDM, a cyclic prefix (CP) and parallel to serial operation(P/S) are employed and then the signals are sent through a frequency-selective Rayleigh fading channel with the channel impulse response (CIR) coefficients

$$h_T = [h(1)\ h(2)\ , \ldots ,\ h(v)]^T , \tag{2}$$

where $h(\sigma)$, for $\sigma = 1, \ldots , v$ follows the circularly symmetric complex Gaussian random distribution $\mathcal{CN}(0, 1/v)$. Assuming that the channel remains constant and the CP length is larger than v, the output of receiver can be presented by

$$y_F(\alpha) = x_F(\alpha)h_F(\alpha) + \omega_F(\alpha),\ \alpha = 1, \ldots , N \tag{3}$$

where $y_F(\alpha)$, $h_F(\alpha)$ and $\omega(\alpha)$ are the received signals, the channel fading coefficients and the noise samples in frequency domain. We assumed that h_0^T is the zero padded version of the vector h_T and therefore $h_F = W_N h_0^T$. It is worth noted that h_F is correlated after FFT operation and W_N is the DFT matrix. The correlation matrix of is given as [12]

$$K = E\left\{h_F h_F^T\right\} = W_N^H \widetilde{\mathrm{I}} W_N \tag{4}$$

where $\widetilde{\mathrm{I}}$ is the $N \times N$ zero matrix except its main diagonal element is a zero padded vector $[\frac{1}{v}, \frac{1}{v}, \ldots , \frac{1}{v}]_{1\times v}$.

B. DIVERSITY ORDER OF OFDM-IM SCHEMES

Due to the K in (4) is a Hermitian Toeplitz matrix, the pairwise error probability (PEP) events within different subblocks are identical. Without loss of generality, we can only analyse the PEP events of a single subblock. Assuming that first subblock X is mistakenly detected as $\hat{X}$, which can be expressed by the conditional PEP (CPEP)

$$\mathrm{P}_C\left(X \to \hat{X}\,|h\right) = Q\left(\sqrt{\frac{\gamma}{2N_{0,F}}}\right) \tag{5}$$

where X is $[x_F(1), \ldots , x_F(n)]^T$, $\hat{X}$ is any other legitimate X and h is the corresponding channel coefficients. Moreover, $\gamma = \left\|\left[\mathrm{diag}\,(X) - \mathrm{diag}(\hat{X})\right] h\right\|_{\mathrm{F}}^2 = h^H A h$ and $A = \left[\mathrm{diag}\,(X) - \mathrm{diag}(\hat{X})\right]^H \left[\mathrm{diag}\,(X) - \mathrm{diag}(\hat{X})\right]$ where $\mathrm{diag}(X)$ is an $n \times n$ all-zero matrix except for its main diagonal elements are X. Afterwards, the unconditional PEP (UPEP) can be achieved by

$$\mathrm{P}_r = E_h\left\{Q\left(\sqrt{\frac{\gamma}{2N_{0,F}}}\right)\right\} \tag{6}$$

where $E_h\{\cdot\}$ is the expectation operation with the channel coefficients h. To further simplify the analysis, the approximate form of Q-function can be given by [30]

$$Q\,(x) \approx \frac{1}{12}e^{-x^2/2} + \frac{1}{4}e^{-2x^2/3} \tag{7}$$

Then the theoretical error performance analysis based on unconditional pairwise error probability (UPEP) calculation is provided by (6) and (7) as [12], thus

$$\mathrm{P}_r\left(X \to \hat{X}\right) = \frac{1/12}{\det\left(\mathrm{I}_n + K_n A/\left(4N_{0,F}\right)\right)} + \frac{1/4}{\det\left(\mathrm{I}_n + K_n A/\left(3N_{0,F}\right)\right)} \tag{8}$$

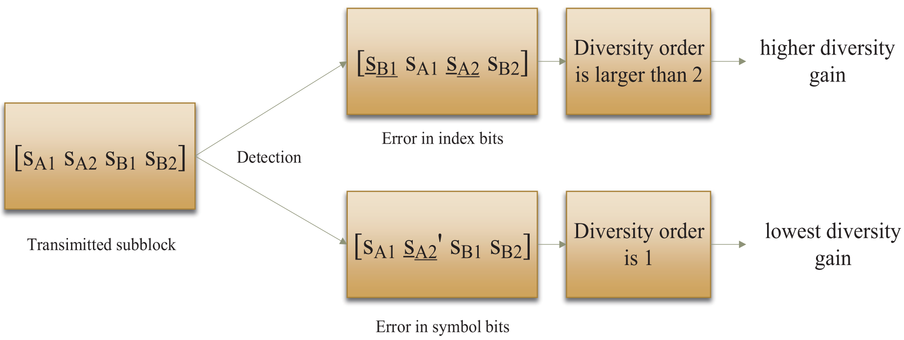

FIGURE 2. Comparison of diversity order between errors in index bits and symbol bits.

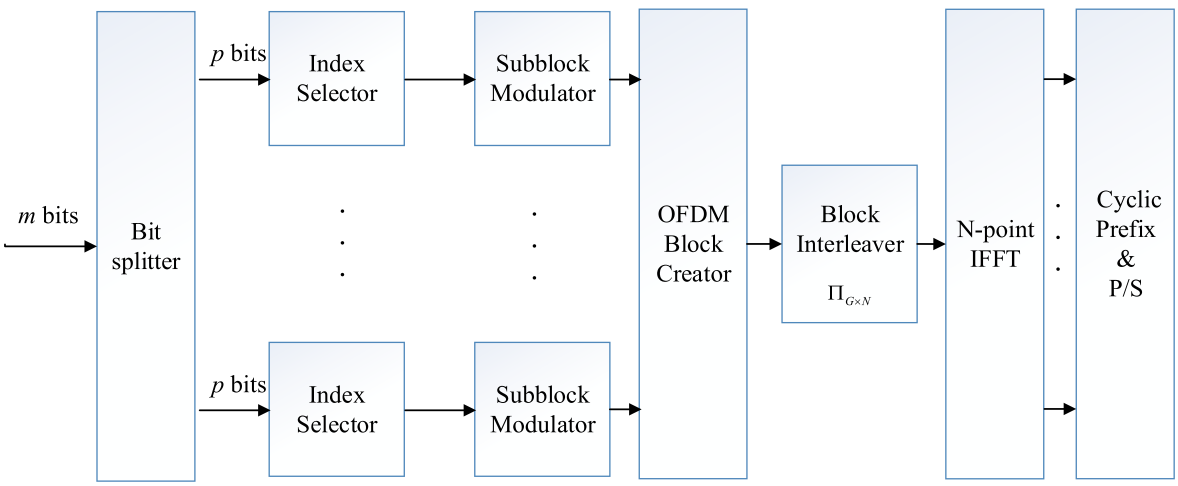

FIGURE 3. The transmitter block diagram of OFDM-AIM.

where K_n is an $n \times n$ submatrix centred along the main diagonal of the matrix K. It is obvious that the UPEP is related to the determinants in denominator, which is predominantly affected by the rank of K_nA. Thus, diversity order of a PEP event can be defined by

$$d = \text{rank}\,(\text{K}_n A) \tag{9}$$

When using a block interleaver, the correlation of channel is removed and $K_n \approx I_n$ [20], and therefore $d = \text{rank}\,(A)$.

The diversity order of index modulated OFDM scheme is depicted in Fig. 2. The errors in index modulated OFDM scheme can be divided into two parts: errors in index bits and in symbol bits. When errors exist in index bits, we calculate that $d \geqslant 2$ due to $s_{B1} \neq s_{A1}$ and $s_{A2} \neq s_{B1}$ (underlined), whilst for symbol bits $d = 1$ with the single error of $s_{A2} \neq s_{A2}{}'$ (underlined), where $s_{A1}, s_{A2}, s_{A2}{}' \in S_A, s_{B1}, s_{B2} \in S_B$, and S_A and S_B are two different constellation alphabets ($S_A \wedge S_B = \emptyset$).

Though the lowest diversity order of OFDM-IM scheme is the same as classical OFDM, it can be seen that the PEP events of index bits can achieve higher diversity order than the symbol bits. Therefore, typical index modulated OFDM schemes enhance the diversity order of systems by replacing a part of symbol bits with the index bits.

However, the diversity gains of the typical index modulated OFDM schemes are still not fully achieved. On the one hand, the typical index modulated OFDM schemes retain the symbol bits, which causes the PEP events with the lowest diversity order. On the other hand, the index modulated OFDM schemes only provide the limited improvement of diversity order ($d \geqslant 2$) for PEP events of index bits. As a result, the subblocks created by typical index modulated OFDM do not focus on the enhancement of diversity gain. To further achieve the diversity gain, we propose the scheme called OFDM with all index modulation (OFDM-AIM), which aims at fully achieving the diversity order of the system.

III. SYSTEM MODEL OF OFDM-AIM

The transmitter diagram is given in Fig. 3. In OFDM-AIM scheme, m-bits are divided into g groups each containing p-bits, namely $m = pg$. Each p-bits are mapping to a certain

TABLE 2. The look-up table of OFDM-AIM.

Index bits	Indices of subblock	Subblock
00	1	X_1
01	2	X_2
10	3	X_3
11	4	X_4

index by index-selector. The function of the index-selector can be represented by a look-up table in Table 2. For incoming $p = 2$bits, the index of the subblock out of four is determined and then the corresponding subblock is modulated by a subblock modulator. Unlike OFDM-IM scheme, we replace the M-ary QAM/PSK modulator with the subblock modulator, which can avoid the transmission of the lowest diversity order symbol bits.

Moreover, the indices of subblock in OFDM-AIM replaces the indices of subcarriers activation patterns of typical index modulated OFDM schemes, which makes the subblocks more flexible. As a result, we can focus on subblocks set design to achieve the potential diversity gain. The selection guideline and algorithm are given in Section IV and Section V.

Assume that the length of OFDM subblock is n and the number of OFDM subcarriers is N, and therefore $N = ng$. After the index selector, the βth subblock containing n OFDM symbols is presented by

$$X_\beta = \left[x_{\beta,1}\ x_{\beta,2}\ ,\ldots,\ x_{\beta,n}\right] \tag{10}$$

where $X_\beta \in \psi$ for ψ is the set of all the legitimate subblocks and $x_{\beta,\gamma}$ is the γth OFDM symbols at βth subblock for $\beta = 1,\ldots,g$ and $\gamma = 1,\ldots,n$. Assuming that the number of subblocks at ψ is N_Ψ, it can be attained that $\log_2(\mathrm{N}_\Psi) = p$ bits and therefore $\mathrm{N}_\Psi = 2^p$.

Then g subblocks are combined at OFDM block creator. After that, a $g \times n$ block interleaver ($\Pi_{g\times n}$) is employed, which is capable of removing the channel correlation. The block interleaver fills the $g \times n$ matrix row by row with the subblocks whilst sends the new interleaved subblocks column by column. As seen from the Fig. 3, the N-point IFFT is conducted and then the addition of a cyclic prefix (CP) is employed. Through the parallel to serial conversion, the signal is sent to the ν-tap frequency selective Rayleigh fading channel.

Before detection at the receiver, the deinterleaver ($\Pi^{-1}_{n\times g} = \Pi_{g\times n}$) is employed to obtain the received signals in frequency domain

$$\mathrm{diag}(Y_\beta) = \mathrm{diag}(X_\beta)\widetilde{h}_\beta + \widetilde{\omega}_\beta \tag{11}$$

where $\mathrm{diag}(X_\beta)$ is $n \times n$ zero matrix except its main diagonal elements are X_β, and $\tilde{h}_\beta$ and $\tilde{\omega}_\beta$ are the decomposed and interleaved inversions of h_F and ω_F for βth subblock. Hence, ML detector can be used to detect the subblock from the legitimate subblocks set, which can be presented by

$$\hat{X}_\beta = \arg\min_{X_\beta}\left\| Y_\beta - X_\beta\tilde{h}_\beta\right\|_2^2 \tag{12}$$

Since X_β has N_Ψ realizaions, the computational complexity is $\sim \mathcal{O}(2^p)$ per subblock. When the SE of the system is not very high, the computational complexity is acceptable.

IV. GUIDELINE TO BUILD LEGITIMATE SUBBLOCKS SET

In this section, we focus on the guideline to build the legitimate set through the analysis of the effect by Euclidean distance and diversity order on PEP. In other words, we demonstrate that the higher diversity gain can be achieved by higher diversity order rather than higher Euclidean distance in most cases.

While using a block interleaver, the correlation of channel is removed and therefore $K_n \approx I_n$ [20]. We rewrite the UPEP in (8), given by

$$\mathrm{P}_r\left(X \to \hat{X}\right) = \frac{1/12}{\det\left(\mathrm{I}_n + A/\left(4N_{0,F}\right)\right)} + \frac{1/4}{\det\left(\mathrm{I}_n + A/\left(3N_{0,F}\right)\right)} \tag{13}$$

To analyse the Euclidean distance between subblocks, the interleaved UPEP can be derived as

$$\begin{aligned}\mathrm{P_r}\left(X \to \hat{X}\right) &= \frac{1}{12}\det\left(\mathrm{I}_n + \frac{1}{4N_{0,F}}\begin{bmatrix}|\Delta s_1|^2 & 0 & 0 & 0\\ 0 & |\Delta s_2|^2 & 0 & 0\\ 0 & 0 & \ddots & 0\\ 0 & 0 & 0 & |\Delta s_n|^2\end{bmatrix}\right)^{-1}\\ &+ \frac{1}{4}\det\left(\mathrm{I}_n + \frac{1}{3N_{0,F}}\begin{bmatrix}|\Delta s_1|^2 & 0 & 0 & 0\\ 0 & |\Delta s_2|^2 & 0 & 0\\ 0 & 0 & \ddots & 0\\ 0 & 0 & 0 & |\Delta s_n|^2\end{bmatrix}\right)^{-1}\end{aligned} \tag{14}$$

where $\Delta s_\delta = \left|x_F(\delta) - \hat{x}_F(\delta)\right|$ is the Euclidean distance at δth OFDM symbol for $\delta = 1,\ldots,n$. Without loss of generality, we assume that $\Delta s_1, \Delta s_2, \ldots, \Delta s_d \neq 0$ and $\Delta s_{d+1}, \Delta s_{d+2}, \ldots, \Delta s_n = 0$ where $d = \mathrm{rank}(A)$ is the diversity order of this UPEP event. Further more, to simplify the analysis, we assume that $\Delta s_1 = \Delta s_2 = \ldots = \Delta s_d = \Delta s \neq 0$, which is the reasonable assumption for worst UPEP events of different diversity orders. Besides, we define $\Delta s^{(d)}$ as a OFDM symbol Euclidean distance of the worst UPEP event with the diversity order d. Thus,

$$\mathrm{P}_r = \frac{1}{12}\left(1 + \frac{\left|\Delta s^{(d)}\right|^2}{4N_{0,F}}\right)^{-d} + \frac{1}{4}\left(1 + \frac{\left|\Delta s^{(d)}\right|^2}{3N_{0,F}}\right)^{-d} \tag{15}$$

At a high SNR region, the value of $N_{0,F}$ can be regarded as $N_{0,F} \ll 1$. Therefore, the simplified form of UPEP can be derived as

$$\mathrm{P}_r \approx \left(\frac{4^d}{12} + \frac{3^d}{4}\right)\left(\frac{N_{0,F}}{\left|\Delta s^{(d)}\right|^2}\right)^d \tag{16}$$

From the formula above, we can evaluate the PEP events of subblocks with different diversity orders represented by d and Euclidean distance presented by $\Delta s^{(d)}$. Considering the effect of diversity order, we calculate that UPEP with diversity order d as P_d, we calculated that $P_{d=1} = 1.08\left(\frac{N_{0,F}}{|\Delta s^{(1)}|^2}\right)$, $P_{d=2} = 3.58\left(\frac{N_{0,F}}{|\Delta s^{(2)}|^2}\right)^2$, $P_{d=3} = 12.08\left(\frac{N_{0,F}}{|\Delta s^{(3)}|^2}\right)^3$ and $P_{d=4} = 41.58\left(\frac{N_{0,F}}{|\Delta s^{(4)}|^2}\right)^4$.

Assuming that $N_{0,F} = 10^{-3}$, which equals to SNR $\approx$ 30dB with normalized signals, the effect of diversity order and Euclidean distance on the UPEP under the frequency selective Rayleigh fading channel with the employment of block interleaver can be seen as Fig. 4. It is observed that the higher diversity order has a great diversity gain on the UPEP performance especially in larger Euclidean distance. For example, when $\Delta s^{(1)}$, $\Delta s^{(2)}$, $\Delta s^{(3)}$ and $\Delta s^{(4)} = 0.5$, $P_{d=4} \approx 10^{-8}$, which is much better than $P_{d=3} \approx 8 \times 10^{-7}$ and $P_{d=2} \approx 6 \times 10^{-5}$ and the diversity gain will disappear gradually as the reduction of Euclidean distance. Hence, it can be indicated that the highest diversity order can achieve the diversity gain when the smallest Euclidean distance between most subblocks is not very small.

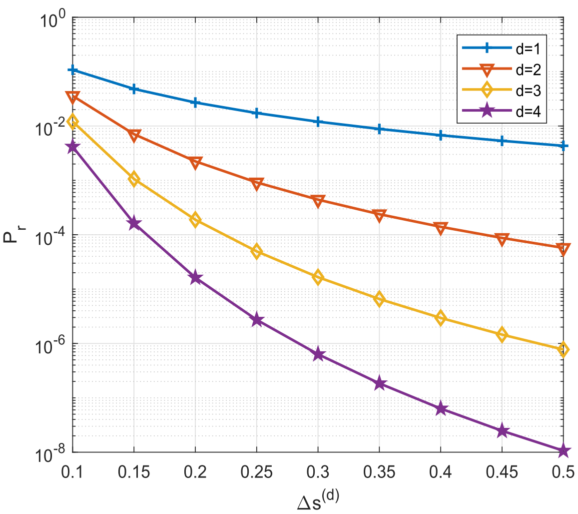

FIGURE 4. **The effect of diversity order and Euclidean distance on the UPEP events.**

Besides, the comparisons in Fig. 4 between the UPEP events with different diversity orders at the same Euclidean distance may not be a fair one because for the UPEP events with $\Delta s^{(4)}$, it means all four OFDM symbols from a subblock have the Euclidean distances of $\Delta s^{(4)}$ compared to the other subblock, while for $\Delta s^{(1)}$, only one OFDM symbol from a subblock has the Euclidean distance of $\Delta s^{(1)}$ compared to the others. Therefore, we focus on the UPEP events at the same UPEP performance with different Euclidean distances and diversity orders to give the relationship between diversity order and Euclidean distance. As is seen from Fig. 5,

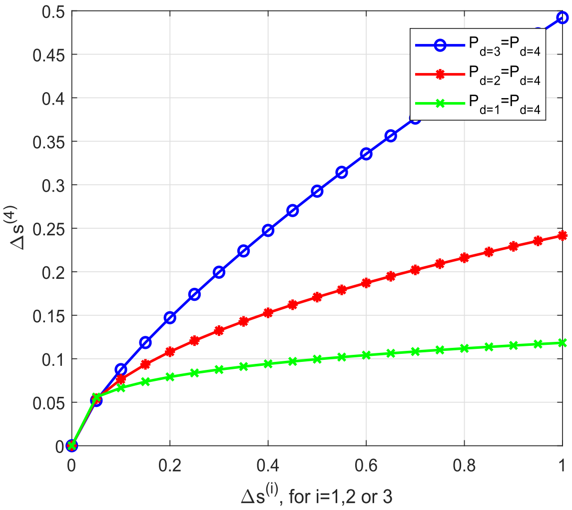

FIGURE 5. **Relationship between subblocks with different diversity order and Euclidean distance at the same UPEP.**

to achieve the same UPEP performance, the subblocks with lower diversity orders are required to attain much higher Euclidean distance. Especially for the curve of $P_{d=1} = P_{d=4}$, it can be seen that even $\Delta s^{(4)} = 0.15$, the highest diversity order introduce much more diversity gain than $\Delta s^{(1)} = 1$. Therefore, we hold the first guideline that we should use the subblocks with the highest diversity order and avoid using the subblocks with the lowest diversity order ($d = 1$). Though the diversity gain of the highest diversity order will disappear when $\Delta s^{(4)} < 0.1$, it worth noted that the smallest Euclidean distance of 16QAM, 64QAM and 256QAM constellations (normalized) are 0.612, 0.306 and 0.153, which still fits the guideline to use the subblocks with the highest diversity order. Moreover, from the curve of $P_{d=3} = P_{d=4}$, it should be noted that the higher diversity order subblocks ($d = 3$) with higher Euclidean distance can also attain better diversity gain, such as the point of $(\Delta s^{(3)}, \Delta s^{(4)}) = (0.4, 0.25)$. Hence, we hold the second guideline that subblocks with higher diversity order ($d = 3$) can also be utilized as the increase of spectral efficiency.

V. THE ALGORITHM OF BUILDING THE LEGITIMATE SUBBLOCKS SET

When the available constellation points of each OFDM symbol set S is determined, and the number of constellation points in set S is N_S, it is obvious that the number of all possible subblocks are N_S^n. Assuming that the number of legitimate subblocks is κ, it is obvious that $\kappa \leqslant N_S^n$. For $\kappa = N_S^n$, it equals to OFDM with the employment of N_S-ary constellation modulation. However, we do not expect the utilization of all symbols combinations due to the low diversity order of system. According to the guidelines in Section IV, we select the subblocks with higher diversity order to build the legitimate subblocks set.

It worth noted that the UPEP events analysis from (13) to (16) is conducted between two legitimate subblocks.

In order to evaluate the BER performance of the system, the average UPEP events (APEP) can be derived as [12]

$$\mathrm{P}_{ave} = \frac{1}{pn_X} \sum_{X \neq \hat{X}} \mathrm{P}_r \left(X \rightarrow \hat{X} \right) \varepsilon \left(X, \hat{X} \right) \quad (17)$$

where $\varepsilon \left(X, \hat{X} \right)$ denotes the number of bit errors in the event that the subblock X is detected as $\hat{X}$ and n_X is the number of the possible realizations of X. Since P_{ave} can be used to approximate the system BER of the OFDM-AIM scheme as an upper bound, it can be also derived by (17) that the BER performance of the system is affected by all possible UPEP events. Hence, every legitimate subblock should keep the higher diversity order to any other legitimate subblocks to achieve the high diversity order of the system.

A simple design to build the highest diversity ($d = n$) subblocks set can be presented as Fig. 6, where the subblocks can be designed as a repeated elements vector. In Fig. 6, when QPSK constellation is employed and the length of subblock $n = 4$, the subblocks with the highest diversity order can be determined. With such arrangement, all of the UPEP events among the legitimate subblocks achieve the highest diversity order. However, the number of subblocks with the highest diversity orders among each other is limited. It is obvious that we can the employ higher order PSK/QAM constellation points to obtain more subblocks with $d = n$.

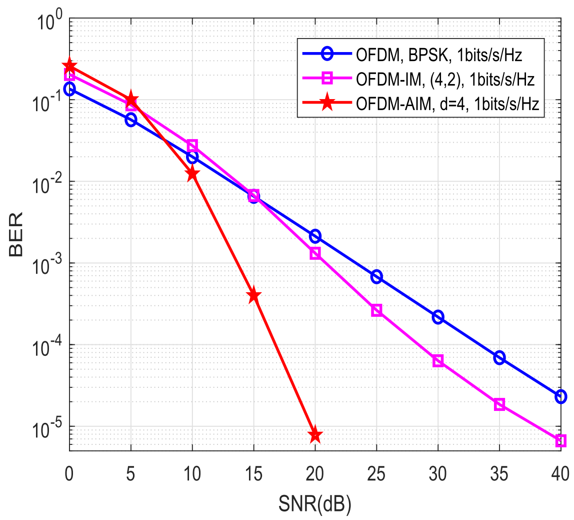

FIGURE 6. The structure of subblocks with the highest diversity order under QPSK constellation points.

Besides, we can also use the subblocks with higher diversity order ($d = n - 1$) as the guideline to increase the spectral efficiency. The algorithm of searching the higher diversity order ($d = n - 1$) subblocks set is given as Algorithm 1.

After obtaining the legitimate set S, which containing κ subblocks, $\lfloor \log_2 \kappa \rfloor$-bits can be conveyed by each subblock. Hence, we can select the first $2^{\lfloor \log_2 \kappa \rfloor}$ subblocks of S as the final legitimate subblocks set. Note that as the increase

Algorithm 1 Search the Higher Diversity Order Subblocks

Input: N_S-ary constellation, length of subblock n. Subblocks with the highest diversity order ($d = n$) are regarded as the inital legitimate subblocks set S. The number of subblocks of inital legitimate subblocks set is κ. $\tilde{X}_i$ is the ith subblock of the legitimate subblocks set. X_j is the jth subblock of all N_S^n possible subblocks.

for $j = 1; j \leqslant N_S^n; j++;$ **do**
  for $i = 1; i \leqslant \kappa; i++;$ **do**
    if rank $\left\{ \mathrm{diag}\left(X_j - \tilde{X}_i\right)^H \cdot \mathrm{diag}\left(X_j - \tilde{X}_i\right) \right\} < n - 1$ **then**
      break;
    end if
    if $i = \kappa$ **then**
      add X_j into S;
      $\kappa++;$
    end if
  end for
end for

Output: legitimate subblocks set S;

of spectral efficiency, we can also add some subblocks with $d = n - 2$, which can be achieved by reusing Algorithm 1.

Moreover, we can introduce more constellation points of each OFDM symbol to expand the search space and therefore more subblocks with higher diversity order can be achieved to increase spectral efficiency.

VI. NUMERICAL RESULTS

In this section, the uncoded BER performance of the OFDM-AIM scheme is compared to conventional OFDM, OFDM-IM [12], DM-OFDM-IM [15], CI-OFDM-IM [20] schemes under the frequency selective Rayleigh fading channel. In all simulations, the length of channel coefficients ν is 10, the number of subcarriers N is 128 and the length of the subblock n is 4. Each BER point is attained by at least 10^5 transmission.

In Fig. 7, the BER performance of the proposed OFDM-AIM based on 16QAM constellation is compared with classical OFDM and OFDM-IM (4,2) employed by BPSK. The spectral efficiencies of OFDM, OFDM-IM (4,2) and OFDM-AIM are both 1 bits/s/Hz. Based on 16QAM constellation search space, 16 repeated vectors are regarded as the legitimate subblocks set, which attains the SE of 1bits/s/Hz. At the BER of 10^{-3}, the simulation results show that the classical OFDM-IM (4,2) has 2dB BER improvement than classical OFDM, which can be explained that the introduction of index bits in OFDM-IM enhances the diversity gain. The proposed OFDM-AIM achieves 10dB and 8dB performance improvement than classical OFDM and the OFDM-IM schemes due to the highest diversity order, which proves the superiority of the proposed scheme.

Fig. 8 depicts the comparison results between classical OFDM, DM-OFDM-IM and OFDM-AIM. Classical OFDM

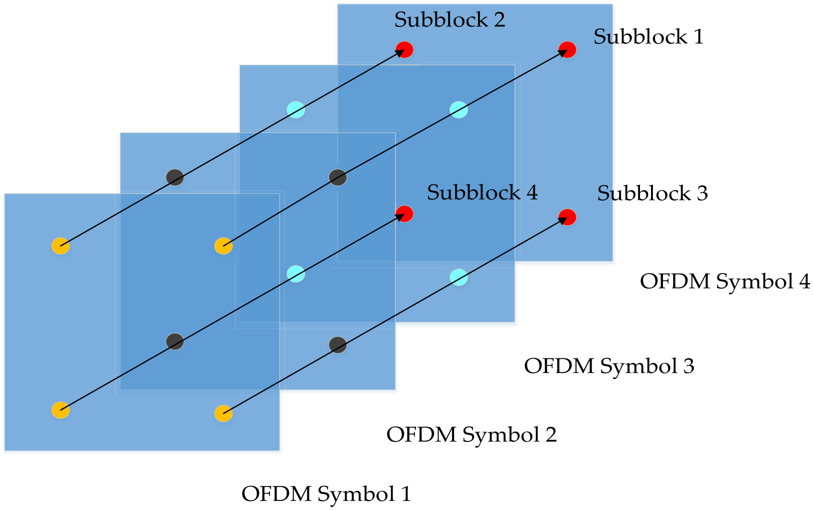

FIGURE 7. Performance comparison among OFDM with BPSK, QPSK and OFDM-AIM with the highest diversity order ($d = 4$) based on 16QAM constellation under frequency selective Rayleigh fading channel.

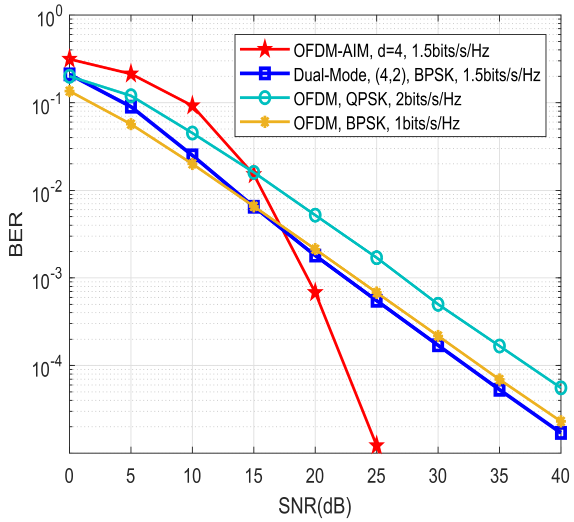

FIGURE 8. Performance comparison among OFDM with BPSK and QPSK, DM-OFDM-IM (4,2), BPSK and OFDM-AIM with the highest diversity order ($d = 4$) based on 64QAM constellation under frequency selective Rayleigh fading channel.

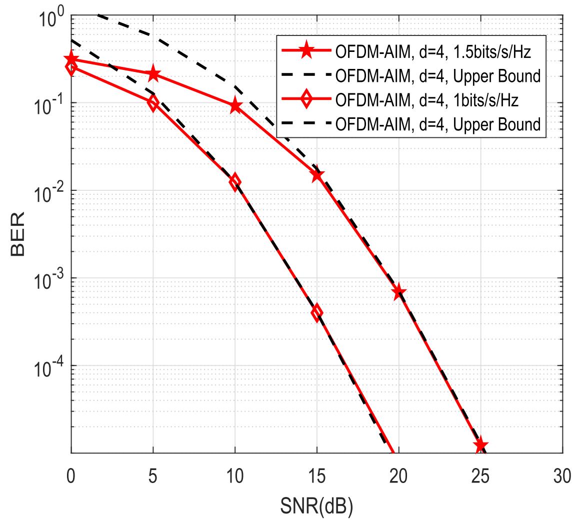

FIGURE 9. Comparison between the theoretical upper bound of OFDM-AIM and the simulated BER performance of the proposed OFDM-AIM with the highest diversity order ($d = 4$) based on 16QAM and 64QAM constellations under the frequency selective Rayleigh fading channel.

schemes with the employment of BPSK and QPSK achieve the SEs of 1 bits/s/Hz and 2 bits/s/Hz. DM-OFDM-IM (4,2) is employed by two distinctive alphabet BPSK sets, which has the SE of 1.5 bits/s/Hz. Based on the search space of 64-QAM constellation points, OFDM-AIM scheme select 64 repeated vector of subblocks achieves the SE of 1.5 bits/s/Hz. At the BER of 10^{-3}, OFDM-AIM scheme achieves about 4dB performance gain than classical OFDM with BPSK and DM-OFDM-IM scheme, and 8dB improvement than OFDM with QPSK. Moreover, as the increase of SNR, the better performance can be achieved by OFDM-AIM due to the highest diversity order.

In Fig. 9, the simulated BER performances of the proposed OFDM-AIM scheme are compared to the corresponding theory analysis results. The average PEP (APEP) based on union bound is used to calculate theoretical upper bound of simulation results. For both the curves with the spectral efficiencies of 1 bits/s/Hz and 1.5 bits/s/Hz, there exists a difference between simulations and theory analysis at low SNR region, which stems from the approximative errors of Q-function.

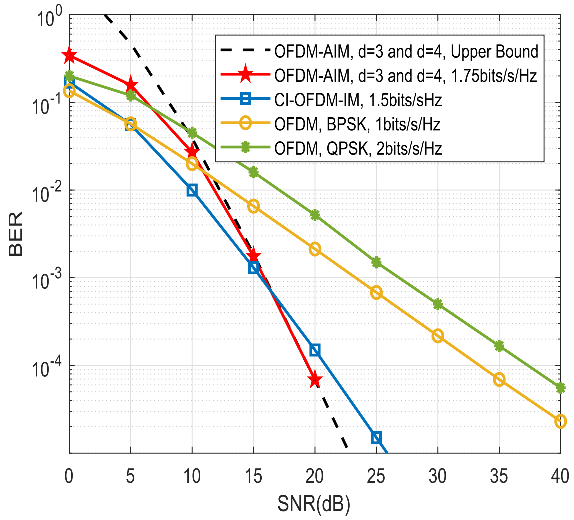

FIGURE 10. Comparison among the theoretical upper bound of OFDM-AIM, the simulated BER performance of OFDM-AIM with higher diversity order ($d = 3$ and $d = 4$) based on 16QAM constellation, CI-OFDM-IM and OFDM with employments of BPSK and QPSK under the frequency selective Rayleigh fading channel.

However, the deviation decrease gradually at medium and high SNR region, which further validates the results of the proposed scheme.

In Fig. 10, the OFDM-AIM scheme employs the subblocks with $d = 3$ and $d = 4$ based on the 16QAM constellation through the algorithm given in Section V. Thus, 199 subblocks which meet the requirement of diversity order are selected out of 65536 subblocks. Then first 128 subblocks are regarded as the legitimate subblocks set to attain the SE of 1.75bits/s/Hz. At BER of 10^{-3}, OFDM-AIM achieves the improvement of 0.25bits/s/Hz spectral efficiency compared to CI-OFDM-IM with almost the same performance. Besides, OFDM-AIM achieves about 7dB and 11dB performance gain compared to classical OFDM with BPSK and QPSK at BER of 10^{-3}. This is because the subblocks set design with higher diversity order in OFDM-AIM scheme, leading to higher diversity gain. Moreover, the theoretical analysis based on union bound is presented, which fits well with the simulative results.

VII. CONCLUSION

A novel scheme called OFDM with all index modulation (OFDM-AIM), which removes the symbol bits of classical OFDM-IM schemes, has been proposed in this paper. The system model of OFDM-AIM is more simple and flexible than index modulated OFDM scheme, which is convenient for subblocks set design. Besides, the relationship of diversity order and Euclidean distance is discussed in our paper, which gives the guidelines that subblocks with higher order should be used to achieve the potential diversity gain. With such arrangement, we propose the simple structure of subblocks set composed by repeated symbols and the algorithm of searching the subblocks with higher diversity order. The theoretical and simulative results demonstrate that the BER performance of OFDM-AIM scheme with proposed subblocks set design outperforms than other index modulated OFDM schemes.

REFERENCES

[1] R. V. Nee and R. Prasad, *OFDM for Wireless Multimedia Communications*. 2000.

[2] D. Astely, E. Dahlman, A. Furuskär, Y. Jading, M. Lindström, and S. Parkvall, "LTE: The evolution of mobile broadband," *IEEE Commun. Mag.*, vol. 47, no. 4, pp. 44–51, Apr. 2009.

[3] F. Adib and D. Katabi, "See through walls with wifi!" *ACM SIGCOMM Comput. Commun. Rev.*, vol. 43, no. 4, pp. 75–86, 2013.

[4] A. Ghosh, D. R. Wolter, J. G. Andrews, and R. Chen, "Broadband wireless access with WiMax/802.16: Current performance benchmarks and future potential," *IEEE Commun. Mag.*, vol. 43, no. 2, pp. 129–136, Feb. 2005.

[5] A. Ghosh, R. Ratasuk, B. Mondal, N. Mangalvedhe, and T. Thomas, "LTE-advanced: Next-generation wireless broadband technology [Invited Paper]," *IEEE Wireless Commun.*, vol. 17, no. 3, pp. 10–22, Jun. 2010.

[6] G. L. Stüber, J. R. Barry, S. W. McLaughlin, Y. Li, M. A. Ingram, and T. G. Pratt, "Broadband MIMO-OFDM wireless communications," *Proc. IEEE*, vol. 92, no. 2, pp. 271–294, Feb. 2004.

[7] E. Basar, M. Wen, R. Mesleh, M. Di Renzo, Y. Xiao, and H. Haas, "Index modulation techniques for next-generation wireless networks," *IEEE Access*, vol. 5, no. 99, pp. 16693–16746, 2017.

[8] T. Mao, Q. Wang, Z. Wang, and S. Chen, "Novel index modulation techniques: A survey," *IEEE Commun. Surveys Tuts.*, vol. 21, no. 1, pp. 315–348, 1st Quart., 2018.

[9] R. Y. Mesleh, H. Haas, S. Sinanovic, C. W. Ahn, and S. Yun, "Spatial modulation," *IEEE Trans. Veh. Technol.*, vol. 57, no. 4, pp. 2228–2241, Jul. 2008.

[10] R. Abu-Alhiga and H. Haas, "Subcarrier-index modulation OFDM," in *Proc. IEEE 20th Int. Symp. Personal, Indoor Mobile Radio Commun.*, Sep. 2009, pp. 177–181.

[11] D. Tsonev, S. Sinanovic, and H. Haas, "Enhanced subcarrier index modulation (SIM) OFDM," in *Proc. IEEE GLOBECOM Workshops*, Dec. 2011, pp. 728–732.

[12] E. Ba ar, U. Aygölü, E. Panayırcı, and H. V. Poor, "Orthogonal frequency division multiplexing with index modulation," *IEEE Trans. Signal Process.*, vol. 61, no. 22, pp. 5536–5549, Nov. 2013.

[13] R. Fan, Y. J. Yu, and Y. L. Guan, "Generalization of orthogonal frequency division multiplexing with index modulation," *IEEE Trans. Wireless Commun.*, vol. 14, no. 10, pp. 5350–5359, Oct. 2015.

[14] B. Zheng, F. Chen, M. Wen, F. Ji, H. Yu, and Y. Liu, "Low-complexity ML detector and performance analysis for OFDM with in-phase/quadrature index modulation," *IEEE Commun. Lett.*, vol. 19, no. 11, pp. 1893–1896, Nov. 2015.

[15] T. Mao, Z. Wang, Q. Wang, S. Chen, and L. Hanzo, "Dual-mode index modulation aided OFDM," *IEEE Access*, vol. 5, pp. 50–60, 2017.

[16] T. Mao, Q. Wang, and Z. Wang, "Generalized dual-mode index modulation aided OFDM," *IEEE Commun. Lett.*, vol. 21, no. 4, pp. 761–764, Apr. 2017.

[17] T. Mao, Q. Wang, J. Quan, and Z. Wang, "Zero-padded orthogonal frequency division multiplexing with index modulation using multiple constellation alphabets," *IEEE Access*, vol. 5, pp. 21168–21178, 2017.

[18] M. Wen, E. Basar, Q. Li, B. Zheng, and M. Zhang, "Multiple-mode orthogonal frequency division multiplexing with index modulation," *IEEE Trans. Commun.*, vol. 65, no. 9, pp. 3892–3906, Sep. 2017.

[19] Y. Xiao, S. Wang, L. Dan, X. Lei, P. Yang, and W. Xiang, "OFDM with interleaved subcarrier-index modulation," *IEEE Commun. Lett.*, vol. 18, no. 8, pp. 1447–1450, Aug. 2014.

[20] E. Ba ar, "OFDM with index modulation using coordinate interleaving," *IEEE Wireless Commun. Lett.*, vol. 4, no. 4, pp. 381–384, Aug. 2015.

[21] M. Wen, X. Cheng, M. Ma, B. Jiao, and H. V. Poor, "On the achievable rate of OFDM with index modulation," *IEEE Trans. Signal Process.*, vol. 64, no. 8, pp. 1919–1932, Apr. 2016.

[22] Z. Liu, Y. Xin, and G. B. Giannakis, "Linear constellation precoding for OFDM with maximum multipath diversity and coding gains," *IEEE Trans. Commun.*, vol. 51, no. 3, pp. 416–427, Mar. 2003.

[23] N. H. Tran, H. H. Nguyen, and T. Le-Ngoc, "Subcarrier grouping for OFDM with linear constellation precoding over multipath fading channels," *IEEE Trans. Veh. Technol.*, vol. 56, no. 6, pp. 3607–3613, Sep. 2007.

[24] M. Wen, B. Ye, E. Basar, Q. Li, and F. Ji, "Enhanced orthogonal frequency division multiplexing with index modulation," *IEEE Trans. Wireless Commun.*, vol. 16, no. 7, pp. 4786–4801, Jul. 2017.
[25] Q. Li, M. Wen, E. Basar, H. V. Poor, B. Zheng, and F. Chen, "Diversity enhancing multiple-mode OFDM with index modulation," *IEEE Trans. Commun.*, vol. 66, no. 8, pp. 3653–3666, Aug. 2018.
[26] J. Choi, "Coded OFDM-IM with transmit diversity," *IEEE Trans. Commun.*, vol. 65, no. 7, pp. 3164–3171, Jul. 2017.
[27] Q. Li, M. Wen, E. Basar, and F. Chen, "Index modulated OFDM spread spectrum," *IEEE Trans. Wireless Commun.*, vol. 17, no. 4, pp. 2360–2374, Apr. 2018.
[28] T. Van Luong, Y. Ko, and J. Choi, "Repeated MCIK-OFDM with enhanced transmit diversity under CSI uncertainty," *IEEE Trans. Wireless Commun.*, vol. 17, no. 6, pp. 4079–4088, Jun. 2018.
[29] T. Van Luong and Y. Ko, "Spread OFDM-IM with precoding matrix and low-complexity detection designs," *IEEE Trans. Veh. Technol.*, vol. 67, no. 12, pp. 11619–11626, Dec. 2018.
[30] M. Chiani and D. Dardari, "Improved exponential bounds and approximation for the Q-function with application to average error probability computation," in *Proc. Global Telecommun. Conf. (GLOBECOM)*, vol. 2, Nov. 2002, pp. 1399–1402.

YUXIN SHI received the B.Sc. degree in communication engineering from the National University of Defense Technology (NUDT), Changsha, Hunan, China, in 2016, where he is currently pursuing the M.Sc. degree with the Department of Communication Engineering, School of Electronic Science. His research interests include index modulation, wireless transmission, and physical layer security.

XINJIN LU received the B.Sc. degree in communication engineering from Hunan University, Changsha, China, in 2016, where she is currently pursuing the M.Sc. degree with the Department of Communication Engineering, School of Electronic Science. Her research interests include channel coding and physical layer security.

KAI GAO received the B.S., M.S., and Ph.D. degrees in electrical engineering from the National University of Defense Technology, Changsha, Hunan, China, in 2000, 2002, and 2006, respectively, where he was a Lecturer in information and communication engineering, from 2006 to 2009 and has also been an Associate Professor in communication engineering, since 2009. He was a Academic Visitor with the University of Strathclyde, U.K., from 2016 to 2017. His current research interests include anti-interference communication, broadband wireless transmission, and communication countermeasures.

JIANG ZHU received the B.S., M.S., and Ph.D. degrees in electrical engineering from the National University of Defense Technology (NUDT), Changsha, Hunan, China, in 1994, 1997, and 2000, respectively, where he was a Lecturer in communication engineering, from 2000 to 2004. He was a Visiting Scholar with the University of Calgary, AB, Canada, from 2004 to 2005. From 2005 to 2008, he was an Associate Professor in communication engineering with NUDT, where he has been a Full Professor with the School of Electronic Science and Engineering, since 2008. His current research interests include wireless high speed communication technology, satellite communication, physical layer security, and wireless sensor networks.

SHILIAN WANG received the B.S. and Ph.D. degrees in information and communication engineering from the National University of Defense Technology (NUDT), China, in 1998 and 2004, respectively.

Since 2004, he has been continuing the research in wireless communications with NUDT, where he later became a Professor. From 2008 to 2009, he was a Visiting Scholar with the Department of Electronic and Electrical Engineering, Columbia University, New York. He is currently the Head of the Laboratory of Advanced Communication Technology, School of Electronic Science, NUDT. He has authored or coauthored two books, 26 journal papers, and 20 conference papers. His research interests include wireless communications and signal processing theory, including chaotic spread spectrum and LPI communications, CPM and STC, underwater acoustic communication and networks, deep learning, and its applications in communication sensing.